Article

Temperature Independence of the Photoinduced Electron Injection in Dye-Sensitized TiO Rationalized by Ab Initio Time-Domain Density Functional Theory

Walter R. Duncan, and Oleg V. Prezhdo

J. Am. Chem. Soc., **2008**, 130 (30), 9756-9762 • DOI: 10.1021/ja800268x • Publication Date (Web): 01 July 2008

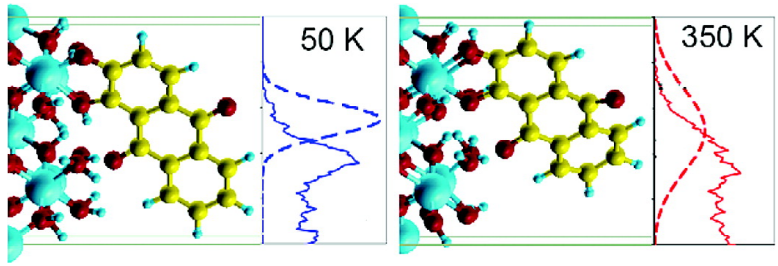

More About This Article

Additional resources and features associated with this article are available within the HTML version:

- Supporting Information
- Access to high resolution figures
- Links to articles and content related to this article
- Copyright permission to reproduce figures and/or text from this article

View the Full Text HTML

J|A|C|S
ARTICLES

Published on Web 07/01/2008

Temperature Independence of the Photoinduced Electron Injection in Dye-Sensitized TiO_2 Rationalized by Ab Initio Time-Domain Density Functional Theory

Walter R. Duncan and Oleg V. Prezhdo*

Department of Chemistry, University of Washington, Seattle, Washington 98195-1700

Received January 12, 2008; E-mail: prezhdo@u.washington.edu

Abstract: Time-domain density functional theory simulations resolve the apparent conflict between the central role that thermal fluctuations play in the photoinduced chromophore−TiO_2 electron transfer (ET) in dye-sensitized semiconductor solar cells [*J. Am. Chem. Soc.* **2005**, *127*, 18234; *Isr. J. Chem.* **2003**, *42*, 213] and the temperature independence of the ET rate [e.g., *Annu. Rev. Phys. Chem.* **2005**, *56*, 119]. The study, performed on the alizarin−TiO_2 interface at a range of temperatures, demonstrates that the ET dynamics, both adiabatic and nonadiabatic (NA), are dependent on the temperature, but only slightly. The adiabatic rate increases with temperature because a fluctuation toward a transition state (TS) becomes more likely. A classical TS theory analysis of the adiabatic ET gives a Gibbs energy of activation that is equal to k_BT at approximately 50 K, and a prefactor that corresponds to multiple ET pathways. The NA rate increases as a result of changes in the distribution of photoexcited-state energies and, hence, in the density of accessible TiO_2 levels, as expressed in the Fermi Golden Rule. In the system under investigation, the photoexcited state lies close to the bottom of the TiO_2 conduction band (CB), and the chromophore−semiconductor coupling is strong, resulting in primarily adiabatic ET. By extrapolating the simulation results to chromophores with excited states deeper inside the CB and weaker donor−acceptor coupling, we conclude that the interfacial ET is essentially independent of temperature, even though thermal ionic motions create a widespread of initial conditions, determine the distribution of injected electron energy, and drive both adiabatic and NA ET.

1. Introduction

The photoinduced electron transfer (ET) between a chromophore and an inorganic semiconductor creates the initial charge separation in the dye-sensitized semiconductor solar cell (DSSC), also known as the Grätzel cell.[1] Many experimentalists[1–15] and theoreticians[2,16–24] have focused on DSSCs because they present a promising alternative to the more costly traditional solar cells made of silicon. They are also remarkably insensitive to temperature change; raising the temperature from 20 to 60 °C has practically no effect on the power conversion efficiency. In contrast, both silicon cells and soft-matter semiconductor cells lose efficiency with increasing temperature.[25]

The conversion of solar energy into an electric current in the DSSC starts with the photoexcitation of the chromophore from its ground state, which is located energetically in the semiconductor band gap, to an excited state that is resonant with the TiO_2 conduction band (CB) (Figure 1). After the excitation, an electron is injected from the chromophore onto the semiconduc-

(1) Oregan, B.; Grätzel, M. *Nature* **1991**, *353*, 737.
(2) Nazeeruddin, M. K.; De Angelis, F.; Fantacci, S.; Selloni, A.; Viscardi, G.; Liska, P.; Ito, S.; Takeru, B.; Grätzel, M. G. *J. Am. Chem. Soc.* **2005**, *127*, 16835–16847.
(3) Snaith, H. J.; Grätzel, M. *Phys. Rev. Lett.* **2007**, *98*, 177402.
(4) Kroeze, J. E.; Hirata, N.; Koops, S.; Nazeeruddin, M. K.; Schmidt-Mende, L.; Grätzel, M.; Durrant, J. R. *J. Am. Chem. Soc.* **2006**, *128*, 16376–16383.
(5) Morandeira, A.; Lopez-Duarte, I.; Martinez-Diaz, M. V.; O'Regan, B.; Shuttle, C.; Haji-Zainulabidin, N. A.; Torres, T.; Palomares, E.; Durrant, J. R. *J. Am. Chem. Soc.* **2007**, *129*, 9250–9251.
(6) Anderson, N. A.; Lian, T. Q. *Annu. Rev. Phys. Chem.* **2005**, *56*, 491.
(7) Asbury, J. B.; Anderson, N. A.; Hao, E.; Ai, X.; Lian, T. *J. Phys. Chem. B* **2003**, *107*, 7376.
(8) Asbury, J. B.; Hao, E.; Wang, Y.; Ghosh, H. N.; Lian, T. Q. *J. Phys. Chem. B* **2001**, *105*, 4545.
(9) Burfeindt, B.; Hannappel, T.; Storck, W.; Willig, F. *J. Phys. Chem.* **1996**, *100*, 16463.
(10) Gundlach, L.; Ernstorfer, R.; Willig, F. *Prog. Surf. Sci.* **2007**, *82*, 355.
(11) Watson, D. F.; Meyer, G. J. *Annu. Rev. Phys. Chem.* **2005**, *56*, 119.
(12) Matylitsky, V. V.; Lenz, M. O.; Wachtveitl, J. *J. Phys. Chem. B* **2006**, *110*, 8372.
(13) Huber, R.; Moser, J. E.; Grätzel, M.; Wachtveitl, J. *J. Phys. Chem. B* **2002**, *106*, 6494.
(14) Huber, R.; Spörlein, S.; Moser, J. E.; Grätzel, M.; Wachtveitl, J. *J. Phys. Chem. B* **2000**, *104*, 8995.
(15) Zhang, D. S.; Downing, J. A.; Knorr, F. J.; McHale, J. L. *J. Phys. Chem. B* **2006**, *110*, 21890.
(16) Paci, I.; Johnson, J. C.; Chen, X. D.; Rana, G.; Popovic, D.; David, D. E.; Nozik, A. J.; Ratner, M. A.; Michl, J. *J. Am. Chem. Soc.* **2006**, *128*, 16546–16553.
(17) Ramakrishna, S.; Willig, F.; May, V. *J. Chem. Phys.* **2001**, *115*, 2743–2756.
(18) Wang, L. X.; Willig, F.; May, V. *J. Chem. Phys.* **2007**, *126*, 134110.
(19) Wang, H.; Thoss, M. *J. Phys. Chem. A* **2003**, *107*, 2126–2136.
(20) Kondov, I.; Cizek, M.; Benesch, C.; Wang, H. B.; Thoss, M. *J. Phys. Chem. C* **2007**, *111*, 11970.
(21) Rego, L. G. C.; Batista, V. S. *J. Am. Chem. Soc.* **2003**, *125*, 7989.
(22) Abuabara, S. G.; Rego, L. G. C.; Batista, V. S. *J. Am. Chem. Soc.* **2005**, *127*, 18234.
(23) Stier, W.; Prezhdo, O. V. *J. Phys. Chem. B* **2002**, *106*, 8047.
(24) Duncan, W. R.; Prezhdo, O. V. *Annu. Rev. Phys. Chem.* **2007**, *58*, 143.
(25) Grätzel, M. *J Photochem. Photobiol. C: Photochem. Rev* **2003**, *4*, 145.

10.1021/ja800268x CCC: $40.75

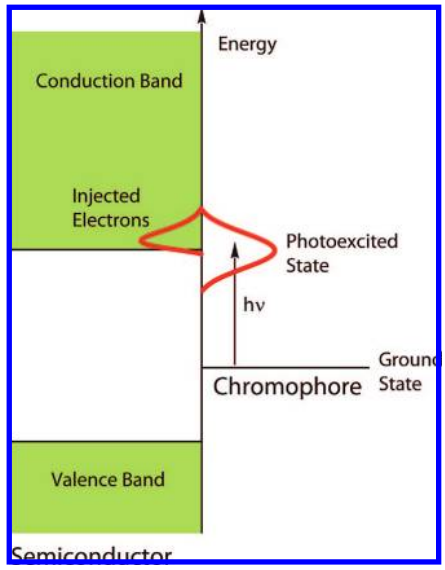

Figure 1. Energy diagram of the alizarin−TiO_2 interface. Thermal vibrational motions create a distribution of the PE electronic-state energies (red Gaussian). PE states with energies below the band edge do not inject the electron until their energy increases above the band edge, which is also due to a vibrational motion. This gives a skewed shape to the injected electron distribution.

tor surface, typically on an ultrafast time scale. The electron then has two different paths open to it: it can complete the cell circuit by delocalizing into the bulk, traveling to the other electrode, and transferring to an electrolyte, which then regenerates the dye ground state, or on the other hand, it can get trapped at the surface and eventually short-circuit the cell by transferring back onto the chromophore or the electrolyte.

ET at the molecular/bulk, organic/inorganic interface is generally a poorly understood process that is nonetheless central not only to the DSSC but also to a number of other developing fields, including molecular electronics,[26,27] photocatalysis,[28–30] photoelectrolysis,[31] and photography.[32,33] A dye that is coupled to TiO_2 offers a good general model for studying ET across such interfaces. In our papers we have characterized the initial ET[34–38,24] in the alizarin system[12–14] and explored the fate of the injected electron.[35,39] An important part of our investigation has been to establish the electron injection mechanism, which determines how changes in the system properties, such as the chromophore and semiconductor energy levels, bridge length, and TiO_2 density of states (DOS), affect the injection process.[6,24] In adiabatic ET, the electron stays in the same electronic state but the localization of that state changes; it moves from the chromophore to the semiconductor as a result of an atomic motion that drives the system over a transition state (TS).[40] In NA ET, the electron quantum-mechanically hops, or tunnels, between electronic states, moving from a state localized on the chromophore to another state with a large localization on the semiconductor. Our study of the alizarin−TiO_2 system has shown that, at ambient temperature, the ET is on average ultrafast (∼10 fs) and primarily adiabatic, with the slower NA mechanism contributing to the process but with a weaker amplitude. An analysis of the individual ET events that make up this average allows us to see the strong influence of atomic motions on the electron injection process.

Zero-temperature calculations show that the photoexcited (PE) state in the alizarin−TiO_2 system is an alizarin state that is located at the CB edge.[37,41] Our NA molecular dynamics (MD) simulations, however, demonstrate that a temperature-induced disorder in the atomic coordinates generates an inhomogeneous distribution of PE states, some of which are well inside the CB and some of which are well below. The nature of the PE state and the subsequent atomic motions dictate the mechanism of ET, in which the states below the CB edge give more NA ET than do those that start far into the CB. Adiabatic ET becomes possible only when an atomic motion changes the energy of the PE state and drives it to a TS. Higher temperatures imply larger amplitude motions and the increased probability of adiabatic ET. The rate of NA ET should also increase with temperature, because the NA coupling is proportional to the atomic velocity. The central role that the thermal motions play, in both creating a distribution of PE states and controlling the injection mechanisms, would seem to imply that changes in temperature should lead to changes in the electron dynamics, including the ET rate.

We have also established the importance of thermal effects in the atomistic simulations performed with other TiO_2−chromophore systems. In our study of isonicotinic acid, the most common ligand in the transition metal chromophores, we determined that the ET changes from adiabatic at ambient temperatures to NA at low temperatures, with a notable decrease in the injection rate.[23,42] Batista and co-workers[22] have also shown a strong connection between ET and temperature. They combined ab initio density functional theory (DFT) MD and the quantum dynamics propagation of transient electronic excitations, using an extended Hückel model Hamiltonian, to study the ET in catechol-sensitized TiO_2. They found that at room temperature the relaxation dynamics were described by a single-exponential decay with a time constant of 2.5 fs. At 0 K, however, there was a 6 fs primary charge separation step and a subsequent 38 fs charge delocalization through the TiO_2

In apparent conflict with both Batista's[22] and our[42] atomistic simulations, which show that thermal atomic motions are very important for the interfacial ET, experimental data indicate not only that DSSC efficiencies are temperature-independent[25] but also that the initial ET is constant over a remarkably large temperature range.[8,9,11] Willig and co-workers[9] performed

(26) Wang, L.; Liu, L.; Chen, W.; Feng, X. P.; Wee, A. T. S. *J. Am. Chem. Soc.* **2007**, *128*, 8003–8007.
(27) Nitzan, A.; Ratner, M. A. *Science* **2003**, *300*, 1384.
(28) Obare, S. O.; Ito, T.; Meyer, G. J. *J. Am. Chem. Soc.* **2006**, *128*, 712–713.
(29) Zhao, W.; Ma, W. H.; Chen, C. C.; Zhao, J. C.; Shuai, Z. G. *J. Am. Chem. Soc.* **2004**, *126*, 4782.
(30) Hirakawa, T.; Whitesell, J. K.; Fox, M. A. *J. Phys. Chem.* **2004**, *108*, 10213.
(31) Lewis, N. S. *J. Electroanal. Chem.* **2001**, *508*, 1–10.
(32) Gould, I. R.; Lenhard, J. R.; Muenter, A. A.; Godleski, S. A.; Farid, S. *J. Am. Chem. Soc.* **2000**, *122*, 11934–11943.
(33) Liu, D.; Hug, G. L.; Kamat, P. V. *J. Phys. Chem.* **1995**, *99*, 16768–16775.
(34) Stier, W.; Duncan, W. R.; Prezhdo, O. V. *Adv. Mater.* **2004**, *16*, 240.
(35) Duncan, W. R.; Stier, W. M.; Prezhdo, O. V. *J. Am. Chem. Soc.* **2005**, *127*, 7941.
(36) Duncan, W. R.; Prezhdo, O. V. *J. Phys. Chem. B* **2005**, *109*, 17998.
(37) Duncan, W. R.; Prezhdo, O. V. *J. Phys. Chem. B* **2005**, *109*, 365.
(38) Craig, C. F.; Duncan, W. R.; Prezhdo, O. V. *Phys. Rev. Lett.* **2005**, *95*, 163001.
(39) Duncan, W. R.; Craig, C. F.; Prezhdo, O. V. *J. Am. Chem. Soc.* **2007**, *129*, 8528.
(40) Memming, R. *Semiconductor Electrochemistry*; Wiley−VCH: Weinheim, Germany, 2001.
(41) Kondov, I.; Wang, H. B.; Thoss, M. *Int. J. Quantum Chem.* **2006**, *106*, 1291.
(42) Stier, W.; Prezhdo, O. V. *Isr. J. Chem.* **2003**, *42*, 213.

transient absorption and fluorescence up-conversion measurements on the interfacial ET between modified perylene chromophores on TiO_2. They found that the dominant ET time constant was independent of temperature; it remained 190 fs from 22 to 300 K.

At the same time, analytic theories of the interfacial ET explain the absence of temperature dependence. Lian and co-workers[6,8] argue that if the coupling between the dye and the semiconductor is strong enough, barrierless ET (transfer that does not require thermal activation) is possible. Strong chromophore−semiconductor coupling implies the adiabatic ET mechanism. In the weak coupling limit, the interfacial transfer becomes NA and depends on the semiconductor DOS rather than an activation barrier. May and co-workers[17,18] argue that in the wide-band limit, which is applicable to the majority of DSSC systems, the DOS is approximately constant over the energies accessible to the chromophore PE state. Assuming that the chromophore−semiconductor coupling is also constant, they deduce that the transfer time is temperature-independent. Thoss and co-workers[19,20] also propose a weak dependence of the ET dynamics on temperature. Their model predicts a very small change in the ET rate over the temperature range from 200 to 500 K. Similarly to Lian and co-workers, they rationalize this prediction by pointing out that the ET occurs near the activationless region, where the crossing between the two electron donor and acceptor surfaces is close to the minimum of the donor surface. By performing a quantum dynamics simulation of the ET process with a model Hamiltonian, the parameters of which are determined by first-principles electronic structure calculations, Thoss and co-workers demonstrate that the ET reaction is not a simple rate process. Rather, quantum interference between the electronic and vibrational degrees of freedom, and between the intramolecular chromophore modes in particular, strongly influences the ET. Therefore, the independence of temperature is quantum-mechanical in nature, an effect similar to quantum tunneling.

The present work reports the first atomistic ab initio time-domain simulation of the interfacial ET over a broad temperature range, addresses the temperature independence of the interfacial ET dynamics, and resolves the apparent conflict between our earlier results, which established the key role of thermally induced vibrational motions,[22,42] with the experimental data and analytical theories showing weak temperature dependence. The study focuses on the ET in the alizarin−TiO_2 system[12–14] from 50 to 350 K. The paper is constructed as follows: The following section describes the essential theoretical background and computational details underlying the NA MD simulation. The results section comprises four parts, focusing on the temperature dependence of the PE-state energy distribution, the adiabatic and NA ET components, and the distribution of the injected electron energies. The simulation results are compared with the available experimental data. The conclusion summarizes the key findings and extends the insights learned with the alizarin−TiO_2 interface to other chromophore−semiconductor systems.

2. Theory

The detailed description of the simulation, which combines time-domain DFT with NA MD, can be found in refs 25, 35, and 39. The simulation closely parallels our earlier work on the alizarin−TiO_2 system at ambient temperature.[24,34–39] The essential details of the simulation procedure and the theoretical approach are summarized below.

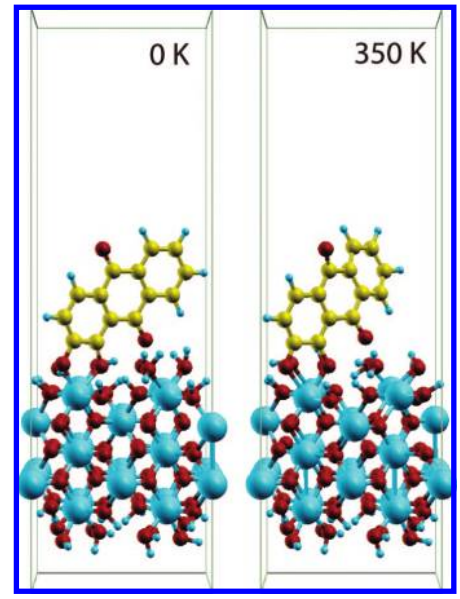

Figure 2. Simulation cell at 0 and 350 K. The optimized structure at 0 K is on the left, and a structure from the 350 K dynamics run is on the right. The positions of the atoms can be notably displaced at this elevated temperature. In particular, distortions of the dye geometry markedly affect the dye-state energies and the PE-state localizations.

2.1. Simulation Details. The majority of the experimental studies of ET in dye-sensitized TiO_2 systems use a mixture of rutile and anatase TiO_2 particles with a variety of surfaces.[43] Water can adsorb on these surfaces both associatively and dissociatively, depending on the type of surface, presence of defects, coverage level, temperature, and other factors.[24,43] Chromophores with multiple binding groups, such as alizarin, can span more than one Ti atom, and they can bond in a bidentate fashion to a single Ti. Since treating all of the possible configurations in a single simulation is computationally infeasible, we focus on a representative system. We chose a single surface of rutile TiO_2, which has a well-defined dissociative interaction with water, and a dissociative bidentate adsorption of alizarin.[41,43,44] The simulation cell, shown in Figure 2, consists of five Ti layers of TiO_2 with water adsorbed on both sides and a single alizarin molecule attached to the top surface. The bottom two layers of the TiO_2 slab are frozen in the bulk configuration. Periodic boundary conditions in three dimensions produce an array of slabs, and the vacuum above and below the surfaces ensures that the slabs do not interact with each other.

The electronic structure and adiabatic MD are computed with the VASP code,[45] using plane wave basis DFT, with the Perdew−Wang-91 density functional[46] and Vanderbilt pseudopotentials.[47] After performing an optimization of the simulation cell geometry, we use velocity rescaling to bring the temperature of the alizarin−TiO_2 system to a given value. We then carry out a 1 ps adiabatic MD simulation in the microcanonical ensemble with a 1 fs time step. The ionic trajectories from this adiabatic MD are then used to sample initial conditions and perform NA MD calculations, which are described below.

2.2. Nonadiabatic Molecular Dynamics with Time-Domain Density Functional Theory. We describe the NA effects in the ET dynamics by time-dependent (TD) DFT within the Kohn−Sham (KS) approach.[23,35,39] The electron density [$\rho(\mathbf{r}, t)$], which is the central quantity in DFT, is expressed within the KS approach by a

(43) Diebold, U. *Surf. Sci. Rep.* **2003**, *48*, 53–229.
(44) Redfern, P. C.; Zapol, P.; Curtiss, L. A.; Rajh, T.; Thurnauer, M. C. *J. Phys. Chem. B* **2003**, *107*, 11419.
(45) Kresse, G.; Furthmüller, J. *Comput. Mater. Sci.* **1996**, *6*, 15.
(46) Perdew, J. P.; Burke, K.; Wang, Y. *Phys. Rev. B* **1996**, *54*, 16533.
(47) Vanderbilt, D. *Phys. Rev. B* **1990**, *41*, 7892.

sum of the occupied KS orbital [$\phi_n(x, t)$] densities. Applying the variational principle to the KS energy gives the evolution of the electron density and produces a set of single-particle equations for the KS orbital evolution:

$$i\hbar\frac{\partial\phi_p(\mathbf{r}, t)}{\partial t} = H(\mathbf{r}, \mathbf{R}, t)\phi_p(\mathbf{r}, t) \quad (1)$$

where $p = 1, 2,..., N_e$. The Hamiltonian depends on time through the external potential created by the ion motion. The equations are coupled by the dependence of the Hamiltonian on the electron density.

We express the TD one-electron wave functions $\phi_p(\mathbf{r}, t)$ in the adiabatic KS basis $\tilde{\phi}_k[\mathbf{r}; \mathbf{R}(t)]$, which is calculated with time-independent DFT, using the atomic positions from the adiabatic MD, described above. The focus is on the evolution of the orbital ϕ_{PE} occupied by the PE electron. As argued previously,[35] the injection dynamics are very well represented by the evolution of the PE electron, which involves the PE molecular orbitals and the TiO_2 CB states, since all other electrons and orbitals are significantly energetically separated from the injected electron. Other states should be included in the simulation only when the longer time dynamics associated with the electron back-transfer are being investigated.[39] The time-dependent KS orbital that is occupied by the PE electron is expanded in the adiabatic KS basis by use of states within the relevant energy range:

$$\phi_{PE}(\mathbf{r}, t) = \sum_k c_k(t)\tilde{\phi}_k[\mathbf{r}; \mathbf{R}(t)] \quad (2)$$

By inserting this expansion into eq 1, we obtain an equation that describes the evolution of the adiabatic state coefficients:

$$i\hbar\frac{\partial}{\partial t}c_j(t) = \sum_k c_k(t)(\epsilon_k\delta_{jk} + d_{jk}) \quad (3)$$

where ϵ_k is the energy of the adiabatic state k and d_{jk} is the NA coupling between KS orbitals k and j, given by

$$d_{jk} = -i\hbar\langle\tilde{\phi}_j|\nabla_{\mathbf{R}}|\tilde{\phi}_k\rangle\frac{d\mathbf{R}}{dt} = -i\hbar\langle\tilde{\phi}_j|\frac{\partial}{\partial t}|\tilde{\phi}_k\rangle \quad (4)$$

By taking the time derivative of the photoexcited electron density expressed in the adiabatic basis, we can find the adiabatic and NA contributions to the ET:[23]

$$\frac{d\int_{dye}\rho_{PE}(\mathbf{r}, t)\,d\mathbf{r}}{dt} = \sum_{i,j}\left\{\frac{d(c_i^*c_j)}{dt}\int_{dye}\tilde{\phi}_i^*\tilde{\phi}_j\,d\mathbf{r} + c_i^*c_j\frac{d\int_{dye}\tilde{\phi}_i^*\tilde{\phi}_j\,d\mathbf{r}}{dt}\right\} \quad (5)$$

The first term has fixed localizations of adiabatic states but changing occupations, while the second term has fixed adiabatic state occupations but changing localizations. These correspond to NA ET and adiabatic ET, respectively. Note that even adiabatic ET can and does involve NA dynamics. In order to be transferred, the PE electron in the molecular state has to find a strongly coupled TiO_2 state by hopping over several uncoupled TiO_2 CB states. The above definition of the NA transfer mechanisms includes this factor by considering only those NA transitions that produce the overall shift of the electron density from the dye onto the semiconductor.

To simulate the ET dynamics in this approach, we first randomly select an initial system geometry from the 1 ps adiabatic MD run. We then determine the PE state at that geometry by finding the adiabatic state with the highest localization on the dye. After calculating the energies and the NA couplings between the states, we propagate the PE electron by solving the above equations with the second order-differencing scheme, using a 10^{-3} fs time-step. The 1 ps adiabatic MD allows us to sample initial conditions for several hundred of these calculations, which we use to determine the average behavior.

3. Results

Thermal motions play a number of roles in the ET dynamics, affecting both the photoexcitation and the subsequent electron injection. The ultrafast ET in the alizarin−TiO_2 system originates in a PE state that is partially delocalized onto the TiO_2 surface. As we have shown in previous papers,[24,34–39] the degree of that delocalization depends on the position of the PE state relative to the CB, as well as on the electronic coupling between the chromophore excited state and the neighboring TiO_2 CB states. Thermal atomic motions modulate both the PE-state energy and the chromophore−semiconductor coupling, thereby changing the nature of the state that is produced by the absorbed photon. Following the excitation, atomic motions continue to play an important role. By causing oscillations in the PE-state energy and bringing the state into and out of the TiO_2 CB, they drive the system through the transition region in an adiabatic transfer. Atomic motions also generate the NA electron−phonon coupling (see the $d\mathbf{R}/dt$ term in eq 4) that is necessary for NA ET. An increase in temperature should, therefore, lead to faster ET for both mechanisms. Finally, the initial spread of the PE-state energy and the subsequent ET dynamics driven by the thermal fluctuations of the atomic coordinates define the distribution of the injected electron energies, which is important in determining the subsequent fate of the electron. It governs, for instance, whether the electron will be able to delocalize into the TiO_2 bulk or remain trapped at the surface. In the following four sections we describe the details of the temperature dependence of the PE-state properties, the adiabatic and NA ET dynamics, and the distribution of the injected electron energies.

3.1. PE Electron Energy Distribution. The kinetic energy present in the system at a finite temperature generates atomic fluctuations around the equilibrium geometry. Figure 2 illustrates the amplitude of the thermal atomic motions. The left and right panels of the figure show the geometry of the alizarin−TiO_2 system in the optimized structure at 0 K and in a random structure from the 350 K trajectory. Note that the bottom two layers of titanium and oxygen atoms, as well as the bottom surface hydroxyl groups, were frozen in the finite temperature simulations, while the top three layers were allowed to move. Upon comparing the zero- and finite-temperature geometries, we observe that the TiO_2 structure changes very little at an increased temperature. The most pronounced changes are seen in the alizarin molecule and in the hydrogens that terminate the top surface.

The chromophore structure influences the energy of the PE state, which is a π^* state delocalized over the carbons and oxygens of the molecule.[14,37,41] In particular, out-of-plane bending distortions perturb the π conjugation and, generally, raise the PE-state energy. This has an enormous effect on the ET process. The PE state of the alizarin−TiO_2 system optimized at 0 K lies below or very close to the edge of the TiO_2 CB.[37,41] This effectively prevents the electron injection in this system from taking place at 0 K. Thermal fluctuations allow the PE-state energy to enter the CB and therefore generate significantly more favorable conditions for ET.

The distribution of the PE-state energies that have been created by the inhomogeneous spread of molecular geometries is plotted by the dashed lines in Figure 3 for 50 and 350 K. The distribution originates from a number of chromophore vibrations and can be well represented by a Gaussian. The range of the state energies that are accessible at the elevated temperatures is significantly broader. The figure also shows the thermally averaged DOS of the TiO_2 CB (solid lines). The DOS features are broadened and smeared out at the higher temperatures, even though the semiconductor atoms move very little.

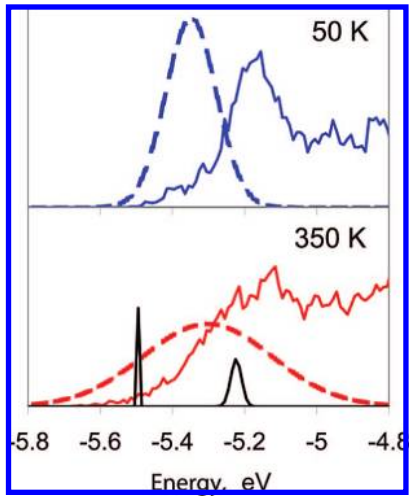

Figure 3. PE-state energy distribution (dashed lines) and TiO_2 DOS (solid lines) for 50 and 300 K, presented in arbitrary linear units as a function of energy. Thermal atomic motions, which create the inhomogeneous distribution of excited-state energies, are larger at higher temperatures. The dye excited state at any fixed geometry is broadened as a result of coupling to the semiconductor states. This homogeneous broadening is shown with black Gaussians for two representative PE states in the 350 K plot. The state at a low energy is below the band edge and does not mix appreciably with the CB states. The higher energy state is in a region with a higher semiconductor DOS and is therefore significantly broadened. Overall, the inhomogeneous broadening is much more substantial than the homogeneous broadening.

Small fluctuations in the TiO_2 coordinates generate disorder in the crystal structure and, in particular, lower the CB edge. Both the broadening of the PE-state energy distribution and the lowering of the CB edge are favorable for the electron injection. At higher temperatures, the PE state is able to interact with a higher density of TiO_2 CB states, facilitating the injection.

As described in detail in some earlier publications,[22,42] thermal atomic motions affect not only the PE-state energy but also the chromophore−semiconductor coupling and, therefore, the extend of delocalization of the PE state onto the semiconductor. At low energies, below the TiO_2 CB edge, the PE state is almost entirely localized on the molecule. At higher energies, inside the CB, the PE state can be strongly localized on the molecule as well. Often, however, the PE state becomes significantly delocalized between the molecule and the semiconductor. The extent of the delocalization depends on the chromophore−semiconductor coupling, which is sensitive to the local details of the geometric structure, including not only the relative positions of the chromophore and semiconductor but also the orientations of the surface hydroxyl groups.[35] Although the PE state can be strongly localized on the chromophore at any energy, generally, at higher energies a larger fraction of the PE state is delocalized on the semiconductor. Therefore, increased temperatures in the alizarin−TiO_2 system raise the contribution of the direct electron injection, in which the electron moves into the TiO_2 surface immediately upon photon absorption.

3.2. Adiabatic ET. The photoinduced electron injection from alizarin into TiO_2 occurs through a combination of adiabatic and NA mechanisms.[35] Our simulation allows us to separate the two contributions by using eq 5. The ET effective rate constant from the simulations, k_{ET}, is determined by fitting the ET data at each temperature to an exponential. Figure 4 presents an Arrhenius plot of $\ln(k_{ET})$ versus $1/T$. With some scatter the

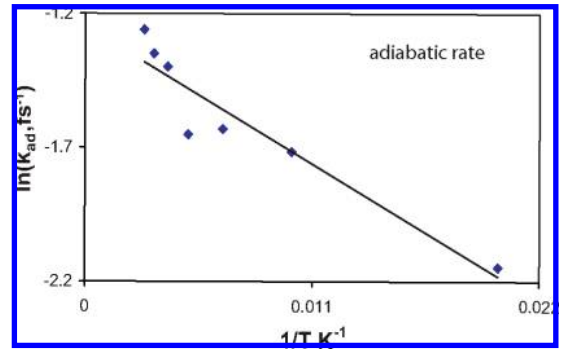

Figure 4. Arrhenius plot of the adiabatic ET data (eq 6). A linear regression of the data gives a Gibbs energy of activation, ΔG, of 4.0×10^{-2} eV and a frequency of nuclear motion, ν, that equals 2.8×10^{14} s^{-1}. The activation energy corresponds to k_BT at approximately 50 K. The frequency of nuclear motion along the ET reaction coordinate is an order of magnitude larger than the frequency of a typical vibrational motion that moves the dye energy into, and out of, the TiO_2 CB. This difference results from the fact that eq 6 represents an effective rate, which is the sum over a number of different ET pathways.

data follow Arrhenius behavior, indicating that the adiabatic injection mechanism can be modeled by use of the traditional expression:

$$k_{ad} = \kappa\nu \exp(\Delta G/kT) \qquad (6)$$

where ΔG is the Gibbs energy of activation, ν is the frequency of nuclear motion through the TS, and κ is a transmission coefficient ranging between 0 and 1, depending on the fraction of trajectories that recross the TS and return the system to the initial state.[40] A linear regression of the data shown in Figure 4 gives a Gibbs energy of activation of 4.0×10^{-2} eV. This is equal to k_BT at approximately 50 K. Higher temperatures would tend to give the system more energy to move through the transition region and over the activation barrier. However, because the calculated energy of activation is so small, our simulations suggest that the adiabatic ET in the alizarin−TiO_2 system should be only weakly dependent on temperature and that the effect of temperature on the injection can be most easily detected by studies carried out below 100 K.

The $\kappa\nu$ prefactor determined by the Arrhenius fit is equal to 2.8×10^{14} s^{-1}. It is reasonable to assume that the transmission coefficient is close to 1 in the present system. There are a large number of bulk TiO_2 states over which the electron can delocalize, but there is only one molecular state to which it can return. The decrease in entropy that is required for the system to recross the TS barrier makes these recrossings very unlikely. Thus, this fitting parameter can be associated with the frequency of the vibrational motion over the TS barrier. The typical vibrational frequencies available in the alizarin−TiO_2 system are on the order of 10^{13}−10^{14} s^{-1}. The fitting parameter exceeds even the highest available frequency, indicating that the adiabatic ET rate constant k_{ad} in eq 6 represents the sum of the individual rate constants for all of the possible reaction pathways. Indeed, multiple TiO_2 surface states couple to the PE state and contribute to the overall ET. The specific TiO_2 state to which the electron transfers at a given nuclear configuration depends on the direction of atomic motion on the multidimensional potential energy surface.

3.3. Nonadiabatic ET. NA ET is the result of direct transition from the dye state to a continuum of conduction band states. In this case, the Fermi Golden Rule can be used to describe the reaction rate:[40]

$$k_{NA} = \frac{2\pi}{\hbar}|V|^2\rho(E_{dye}) \quad (7)$$

where V is the donor−acceptor coupling, and $\rho(E_{dye})$ is the semiconductor DOS at the energy of the dye PE state, E_{dye}. Increased temperatures will push the energy of the dye state higher into the CB, where the DOS is larger, leading to a faster transfer.

The NA ET simulation data for each temperature were fit to an exponential in order to get the rate constant for NA ET. In order to apply eq 7 to the rate constants from the simulations, we defined an average density of TiO_2 states that interact with the dye. The average takes into account the fact that thermal vibrational motions modulate the PE-state energy, making it fluctuate by several tenths of an electronvolt and interact with different regions of the TiO_2 DOS. As demonstrated in Figure 3, the TiO_2 DOS varies significantly over the PE-state energy range that is generated by the atomic motions. The average DOS entering eq 7 was computed for each temperature by multiplying the PE-state energy distribution by the TiO_2 DOS and integrating over the energy. As expected, this average accessible DOS tends to increase with temperature.

A plot of the NA ET rates versus the average TiO_2 DOS with which the dye can interact is shown in Figure 5. Assuming a constant value of the chromophore−semiconductor coupling, this plot should, according to the Fermi Golden Rule, be linear (eq 7). It clearly is not, but it does show a general trend of increasing transfer rate with increasing DOS. The nonlinearity most likely results from the fact that the coupling between the dye and semiconductor states is not constant and varies with both energy and time. Additional scatter in the data arises because the NA transfer is a minor component of the overall ET,[35] limiting the statistical convergence. The relative changes in the NA ET rate are of the same order of magnitude, about a factor of 2 over the considered temperature range, as the changes in the adiabatic ET rate (Figure 4). While the contribution of the NA ET mechanisms increases with decreasing temperature, the adiabatic ET dominates the overall dynamics at both high and low temperatures.

3.4. Injected Electron Energy Distribution. As discussed above, thermal vibrational motions affect the ET dynamics by generating a distribution of initial conditions for the ET and by driving both the adiabatic and NA processes. The injected

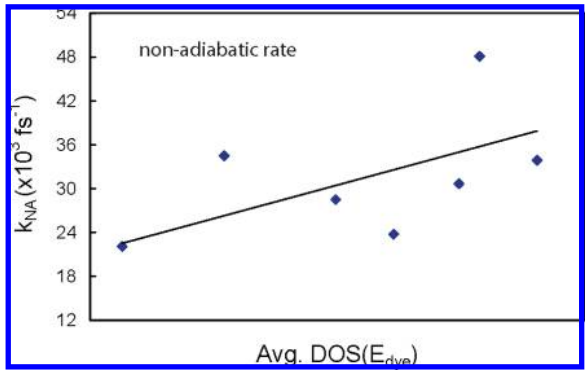

Figure 5. Nonadiabatic ET rate constant, k_{NA}, as a function of the available TiO_2 DOS, $\rho(E_{dye})$, eq 7, given in arbitrary linear units. The available DOS is obtained by integrating over the TiO_2 DOS with the weight that is given by the dye-energy distribution, both of which are shown in Figure 3. The plot shows a general trend of increasing NA transfer rate with increasing DOS, and therefore with increasing temperature. The scatter in the data arises from the fact that the coupling between the dye and semiconductor states, V in eq 7, is not constant.

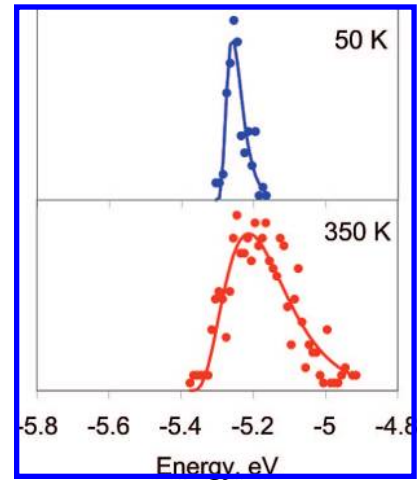

Figure 6. Distributions of the injected electron energies for 50 and 350 K, presented in arbitrary linear units as a function of energy. The data are to be compared with the distributions of the PE electron energies shown in Figure 3. The injected electron distribution is skewed, because the PE states that are below the band edge do not inject the electron until an atomic motion brings their energy inside the TiO_2 CB. As established earlier,[35] atomic motions modulate the PE-state energy much more than the CB edge energy. Therefore, both PE-state and injected electron energy distributions are wider at elevated temperatures.

electrons create an energy distribution that can be detected experimentally.[48,49] Since the injection occurs significantly faster than any type of relaxation, including that inside the molecule and inside the semiconductor, the injected electron distribution is entirely determined by the PE-state distribution and the ET process. The ET is essentially isoenergetic relative to the spread of the PE-state distribution (Figure 3). Large NA jumps in energy are unlikely, and finding an adiabatic TS does not require a big energy fluctuation. The PE states that are below the TiO_2 CB constitute the only exception. They have to be brought inside the CB by a fluctuation in order for the ET to take place. Therefore, the distributions of the injected electron energy mirror the PE-state distributions at high energies and are skewed at the lower energies, where the TiO_2 DOS is 0. This explains the pulselike shape of the injected electron energy distributions shown in Figure 6. Similar to the dashed Gaussians in Figure 3, the skewed Gaussian in Figure 6 is significantly more narrow at 50 K than at 350 K.

Willig and co-workers[48] measured the energy distribution of the electrons that were injected from perylene into TiO_2 using two-photon photoemission. In contrast to the alizarin system, whose PE state is near the CB edge, they found that the first excited state of perylene is approximately 0.5 eV above the CB edge. At this energy, the DOS is relatively constant and sufficiently high that the transfer can happen as soon as the excited state is occupied. The high density of acceptor states at the excited dye-state energy leads to substantial state mixing and creates a spread over at least 1 eV in energy. Willig and co-workers suggested that these acceptor states are surface states that result from the formation of chemical bonds between the dye anchor groups and the surface atoms of the semiconductor. They performed similar experiments with catechol, which also established injected energy distributions on the order of 1 eV.[48,49] These distributions are notably broader than what we

(48) Persson, P.; Lundqvist, M. J.; Ernstorfer, R.; Goddard, W. A., III; Willig, F. *J. Chem. Theor. Comput.* **2006**, *2*, 441–451.
(49) Gundlach, L.; Ernstorfer, R.; Willig, F. *Phys. Rev. B* **2006**, *74*, 035324.

see with alizarin. The difference arises from a number of factors. First, the distributions of the injected electron energies in the alizarin−TiO_2 system are cut nearly in half relative to those expected if the alizarin PE state were deep inside the TiO_2 CB. Second, the experimental data should definitely exhibit a larger degree of inhomogeneous broadening. Our simulation cell has only one perfect surface and a single chromophore bound to the surface in one of the possible conformations. The real system has a mixture of surfaces and chromophore−TiO_2 bonding conformations, as well as several types of surface defects, such as atom vacancies, step edges, and impurities. We believe that the additional degree of inhomogeneity is responsible for a similar relationship between our PE-state distribution and the bandwidth of the experimental spectrum of alizarin bound to TiO_2.[14] The experimental width at half-maximum is about 0.7 eV, while our distribution is a little more than half that, 0.4 eV (Figure 3).

4. Discussion and Conclusions

One advantage of DSSCs is that their performance is remarkably temperature-independent.[25] Previous atomistic simulations have shown, however, that thermal motions play a central role in determining the ET dynamics.[22,35,39,42] We have rationalized that apparent conflict by performing NA MD simulations on the alizarin−TiO_2 system at a series of temperatures ranging from 50 to 350 K. Our results show that the ET is indeed driven by vibrational motions and that both adiabatic and NA ET are sped up at increased temperatures. However, the temperature dependence is minor; the rate changes only by a factor of 2 over this wide temperature region. The adiabatic mechanism involves transition over a barrier. Additional thermal kinetic energy favors this transition. The effective barrier height in the alizarin−TiO_2 system corresponds to k_BT at 50 K. Therefore, at temperatures above 100 K the adiabatic transfer becomes essentially barrierless, and any amount of vibrational motion is sufficient to induce the transfer. The NA mechanism depends on electron−phonon coupling that results from nuclear kinetic energy. Efficient NA transfer is facilitated by a high density of acceptor states. Elevated temperatures increase the coupling and introduce a disorder that raises the average energy of the PE state, putting it deeper inside the TiO_2 CB. As with the adiabatic transfer, the change in the NA ET rate is minor, a factor of 2 between 50 and 350 K, once again because even a small NA coupling generates efficient transfer in the presence of a high density of acceptor states.

The key conclusions of our work hold both for organic chromophores and for transition-metal/ligand complexes. As is the case with an organic chromophore, the PE state of a transition metal complex is a π^* orbital. The electron donor−acceptor coupling is identical in the two chromophore types and involves interaction between d orbitals of the Ti atoms and the π^* orbital. The thermal atomic motions discussed in this paper are primarily those of the dye/ligand and show little contribution from the semiconductor. Therefore, the reported results should not be sensitive to a specific choice of the TiO_2 surface. Previously, we modeled the isonicotinic acid ligand with[42] and without[23] a transition metal. The study showed little dependence of the injection process on the presence of the metal, and the ligand vibrational motions drove the injection even with the metal present. Batista and co-workers[22] studied catechol on anatase TiO_2, in contrast to rutile TiO_2, which was used in the present work, and also observed the importance of the thermal atomic motions. Thus, the findings reported here regarding the role of thermal atomic motions and the temperature-independence of the injection rate are valid regardless of the sensitizer dye and the TiO_2 surface and provide useful information for the improvement of the DSSCs.

Extending the conclusions obtained with our atomistic simulation of the alizarin−TiO_2 system to other molecule−semiconductor interfaces, we note that the present system is a somewhat special case and that the temperature effects should be even less pronounced for an average interface. The PE state of alizarin lies close to the edge of the TiO_2 CB. This condition creates a minor barrier to the adiabatic ET and positions a fraction of the PE-state distribution in the low TiO_2 DOS region. As pointed out previously, this configuration can be useful in practice since it avoids the energy losses that are associated with electron injection higher in the CB. In a typical DSSC system, the PE state is well inside the CB, in the region where the acceptor DOS is already high and where an adiabatic TS can be found by moving not only uphill but also downhill in energy. This configuration requires very little thermal energy to initiate the electron injection, as observed in the experiments[8,9,11,25] and predicted by the analytic theories.[6,8,17–20]

Similar considerations can explain the observation of temperature-independent back-ET from TiO_2 to the chromophore ground state, which results in a loss of efficiency in DSSCs.[50] Since the gap between the bottom of the TiO_2 CB and the chromophore ground state is large, adiabatic ET requires crossing a huge barrier in the inverted Marcus region and it is essentially impossible. The atomistic simulation confirms that the back-ET occurs by the NA mechanism.[1] The density of acceptor states is constant, since it is the chromophore ground state. Thermal effects enter only the NA coupling matrix element, eq 4 via the nuclear velocity $d\mathbf{R}/dt$. According to the Fermi Golden Rule (eq 7), the rate of NA transfer is proportional to the square of the coupling and, therefore, to the square of the nuclear velocity and the first power of kinetic energy and temperature. Varying the temperature between 250 and 350 K, for instance, will change the back-ET rate only by 350/250 = 1.4, which constitutes a minor effect relative to the changes in rate that are induced by variations in TiO_2 surfaces, chromophore−semiconductor binding, surface defects, solvent, etc.

In summary, the results of our atomistic simulations provide a clear and straightforward explanation of the experimentally observed insensitivity of the interfacial ET processes in the DSSC systems to temperature. While ET is promoted by atomic vibrational motions, and therefore the ET rates do depend on temperature, the dependence is very minor relative to other experimental factors.

Acknowledgment. The research was supported by grants from NSF CHE-0701517 and ACS-PRF 46772-AC6.

JA800268X

(50) Moser, J. E.; Grätzel, M. *Chem. Phys.* **1993**, *176*, 493.